Developmental Cell
Short Article

Gene Regulation by MAPK Substrate Competition

Yoosik Kim,[1] María José Andreu,[2] Bomyi Lim,[1] Kwanghun Chung,[3] Mark Terayama,[4] Gerardo Jiménez,[2] Celeste A. Berg,[4] Hang Lu,[3] and Stanislav Y. Shvartsman[1,*]
[1]Department of Chemical and Biological Engineering and Lewis-Sigler Institute for Integrative Genomics, Princeton University, Princeton, NJ 08544, USA
[2]Institut de Biologia Molecular de Barcelona-CSIC and Institució Catalana de Recerca i, Estudis Avançats, Parc Científic de Barcelona, Barcelona 08028, Spain
[3]School of Chemical and Biomolecular Engineering and Parker H. Petit Institute for Bioengineering and Bioscience, Georgia Institute of Technology, Atlanta, GA 30332, USA
[4]Department of Genome Sciences, University of Washington, Seattle, WA 98195-5065, USA
*Correspondence: stas@princeton.edu
DOI 10.1016/j.devcel.2011.05.009

SUMMARY

Developing tissues are patterned by coordinated activities of signaling systems, which can be integrated by a regulatory region of a gene that binds multiple transcription factors or by a transcription factor that is modified by multiple enzymes. Based on a combination of genetic and imaging experiments in the early *Drosophila* embryo, we describe a signal integration mechanism that cannot be reduced to a single gene regulatory element or a single transcription factor. This mechanism relies on an enzymatic network formed by mitogen-activated protein kinase (MAPK) and its substrates. Specifically, anteriorly localized MAPK substrates, such as Bicoid, antagonize MAPK-dependent downregulation of Capicua, a repressor that is involved in gene regulation along the dorsoventral axis of the embryo. MAPK substrate competition provides a basis for ternary interaction of the anterior, dorsoventral, and terminal patterning systems. A mathematical model of this interaction can explain gene expression patterns with both anteroposterior and dorsoventral polarities.

INTRODUCTION

Similar to other multicellular organisms, *Drosophila* uses its extracellular signal-regulated kinase/mitogen-activated protein kinase (ERK/MAPK) pathway throughout embryogenesis. It is first used downstream of Torso receptor tyrosine kinase (RTK), to specify the nonsegmented terminal regions of the future larva. Locally activated Torso establishes a two-peaked pattern of activated, double-phosphorylated ERK/MAPK (dpERK) (Coppey et al., 2008; Gabay et al., 1997). One MAPK substrate is an HMG-box transcriptional repressor Capicua (Cic), which is uniformly expressed in the embryo (Jiménez et al., 2000). In a process essential for the development of the terminal structures, Cic is degraded at the poles in direct response to its phosphorylation by MAPK (Ajuria et al., 2011; Astigarraga et al., 2007; Jiménez et al., 2000). Another substrate of MAPK is an anteriorly localized homeodomain protein Bicoid (Bcd), which determines the anterior pattern of the embryo (Janody et al., 2000; Ronchi et al., 1993).

Together with another anteriorly localized MAPK substrate, Hunchback (Hb), Bcd antagonizes MAPK-dependent downregulation of Cic (Kim et al., 2010). Our earlier work supports a model whereby MAPK substrates indirectly affect each other by competing for their common regulator (Kim et al., 2010). Competitive effects of this type should be common in large-scale biomolecular networks where one regulator controls a large number of targets. Computational studies of mass-action networks demonstrate that, in general, competitive effects decay with distance (the number of interaction edges) from perturbed nodes (Maslov and Ispolatov, 2007). In other words, competitive effects could be localized to a specific node and thus might not significantly affect more distant network components. In the context of the terminal patterning system, anteriorly localized MAPK substrates can decrease the level of Cic downregulation, but the effect may be too small to impact Cic-dependent gene regulation.

Here, we present evidence to the contrary and propose that MAPK substrate competition controls gene expression in the early embryo. This conclusion is based on the analysis of the expression pattern of *zerknüllt* (*zen*), which encodes a homeodomain transcription factor and is expressed in a complex pattern that depends on the joint action of the terminal and dorsoventral (DV) patterning systems (Figure 1). *zen* expression is broadly activated by Zelda and possibly other maternal factors, and repressed in the ventral and lateral regions by Dorsal (Dl), a transcription factor that patterns the DV axis (Figures 1A and 1B) (Doyle et al., 1989; Jiang et al., 1993; Liang et al., 2008; Ratnaparkhi et al., 2006). At the poles, Dl-mediated repression of *zen* is antagonized by Torso signaling (Rusch and Levine, 1994).

The precise mechanism of *zen* derepression by the terminal system has been unclear, but it is likely to depend on MAPK-dependent downregulation of Cic (Astigarraga et al., 2007; Goff et al., 2001; Jiménez et al., 2000). We demonstrate that the antirepressive effect of MAPK signaling on *zen* is modulated by the anteriorly localized MAPK substrates. Specifically, removing anterior MAPK substrates makes *zen* expression symmetric along the anteroposterior (AP) axis. Our results support a mechanism whereby MAPK substrate competition controls spatial patterns of gene expression by coordinating the actions of the anterior, DV, and terminal systems. We formalize this mechanism in a mathematical

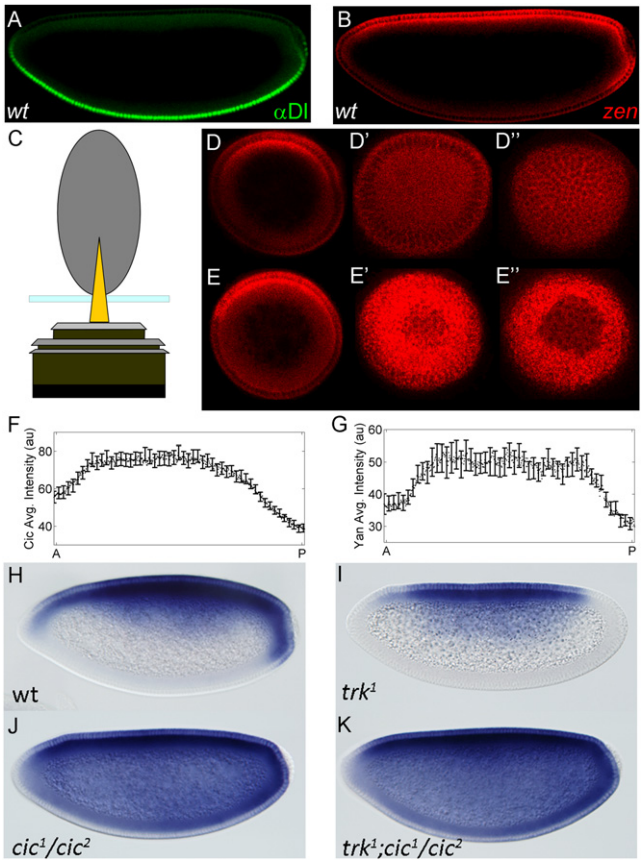

Figure 1. Expression of *zen* mRNA Exhibits AP Asymmetry

(A and B) Spatial patterns of Dl protein (green) and *zen* mRNA (red) in a wild-type embryo. *zen* transcripts were detected by FISH (see Experimental Procedures). The image is oriented with anterior left and dorsal side up.

(C) Schematic of end-on imaging.

(D) Optical sections of an embryo stained with *zen* mRNA at ~70 μm (D), ~7 μm (D′), and 0 μm from the anterior pole (D″). These images are oriented with the dorsal side up.

(E) *zen* expression at the posterior pole: optical sections at ~70 μm (E), ~7 μm (E′), and 0 μm from the posterior pole (E″).

(F) AP gradient of nuclear Cic in wild-type embryos. Solid line is the average gradient, based on 29 embryos. Error bars indicate standard error of the mean (SEM). The nuclear level of Cic is significantly higher at the anterior pole, suggesting weaker MAPK enzymatic activity in this region ($p < 0.001$).

(G) Enzymatic activity of MAPK can also be assessed by quantifying the spatial pattern of ectopically expressed Yan. Similar to Cic, Yan downregulation by MAPK is significantly weaker in the anterior region ($p < 0.001$). Solid line is the average gradient, based on 23 embryos; error bars indicate SEM.

(H–K) *zen* mRNA in a wild-type embryo (H), *trk* embryo (I), *cic* embryo (J), and *trk cic* double-mutant embryo (K). *zen* transcripts are detected using alkaline phosphatase staining.

model and demonstrate that this model correctly predicts *zen* expression in multiple genetic backgrounds.

RESULTS

Cic Downregulation Is Required for *zen* Expression at the Poles

zen expression pattern displays a pronounced AP asymmetry: *zen* transcripts are present at the posterior but not at the anterior pole. This asymmetry is particularly clear when embryos are imaged in an upright position (Figure 1C). As shown in Figures 1D and 1E, *zen* transcript levels are markedly different at the anterior versus the posterior pole of the embryo. Below, we argue that AP asymmetry of *zen* expression can be explained by a mechanism that relies on MAPK substrate competition. Briefly, we propose that MAPK-dependent downregulation of Cic is responsible for *zen* derepression at the poles. Anteriorly localized MAPK substrates inhibit Cic downregulation, increasing the level of Cic and thus the strength of Dl-dependent *zen* repression at the anterior pole.

As a first step in evaluating this model, we asked whether Cic downregulation by Torso signaling contributes to *zen* expression at the poles of the embryo. Previous studies (Jiménez et al., 2000; Astigarraga et al., 2007) suggested that Cic is involved in Dl-dependent ventral repression of *zen* (Figures 1H–1J). To test whether downregulation of Cic is also involved in Torso-dependent control of *zen* at the poles, we examined *zen* expression in embryos derived from *trunk* (*trk*) and *cic* double-mutant females. *trk* encodes a Torso ligand, which is required for MAPK activation at the poles (Casanova et al., 1995) as well as the posterior expression of *zen* (Figure 1I). If the latter effect is due to the lack of Cic downregulation, then posterior expression of *zen* should be restored in embryos that lack both Cic and Trk. Consistent with this prediction, we found that *zen* is significantly derepressed in embryos derived from *trk cic* double-mutant flies (Figure 1K).

Taken together with the results of previous studies, our data support a model where Cic downregulation is necessary for *zen* expression at the poles. Based on the previously characterized AP asymmetry of Cic downregulation (Figure 1F), we propose that higher levels of Cic at the anterior pole are responsible, at least in part, for reduced expression of *zen* in this region. We found that both of these asymmetries are seen in other *Drosophilids* (see Figure S1 available online), suggesting that the proposed mechanism is conserved and might be functionally significant.

Mathematical Model Describes *zen* Expression

Based on the above results, we formulated a mathematical model of *zen* regulation: *zen* is activated by spatially uniform activators, such as Zelda (U), and repressed by the ventral-to-dorsal nuclear gradient of Dl. Repression of *zen* by Dl requires a cofactor (R), which is downregulated at the poles by the terminal signal (E, which models locally activated MAPK). At the anterior pole, the enzymatic activity of E toward R is inhibited by the anteriorly localized substrates of E (B, which models the combined effects of Bcd and Hb) (Figure 2B). In the simplest case, R can be viewed as Cic, which is clearly involved in Dl-dependent *zen* repression (Figure 1).

We note that our model does not rely on the assumption that Cic is the only MAPK substrate required for Dl-dependent repression of *zen* (Dubnicoff et al., 1997; Jiang et al., 1993; Jiménez et al., 2000). Thus, R can represent a collective effect of spatially uniform MAPK substrates that are involved in Dl-dependent *zen* repression. We expect that these substrates, some of which are yet to be identified, will also be subject to competitive effects of anteriorly localized MAPK substrates. This idea is supported by the following experiment, which used nuclear

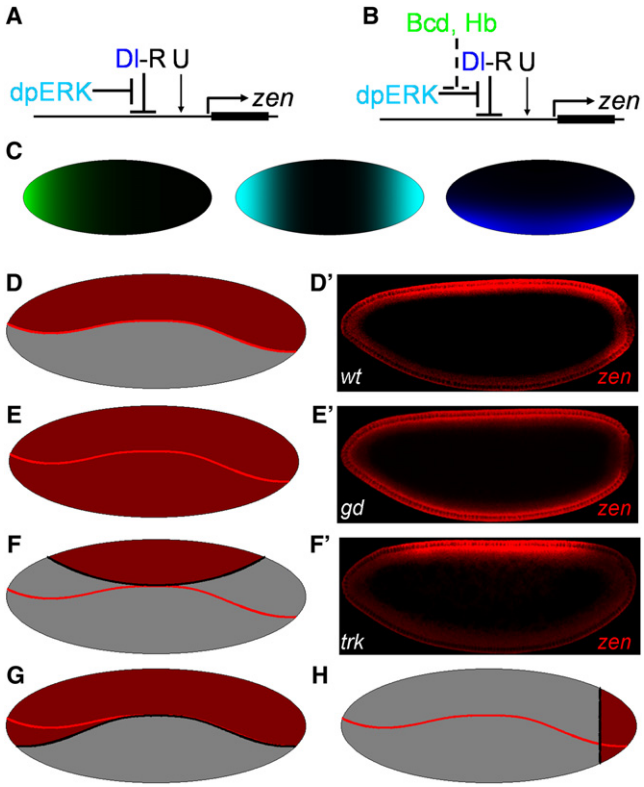

Figure 2. Mathematical Model of *zen* Regulation by MAPK Substrate Competition

(A) A model for the early pattern of *zen* expression (Rusch and Levine, 1994): *zen* is induced by uniform activators (U) and repressed in the ventral region of the embryo by the nuclear Dl gradient (Dl-R). Dl-mediated repression is antagonized at the poles by MAPK.

(B) Revised model: the anteriorly localized substrates of MAPK (Bcd, Hb) competitively inhibit MAPK-mediated *zen* derepression.

(C) Schematic representation of the spatial distribution of maternal factors contributing to the regulation of *zen*: Bcd+Hb (green), dpERK (cyan), and Dl (blue).

(D–F′) The model successfully predicts *zen* expression in mutants. The boundary of the wild-type pattern is indicated by a solid red line. *zen* in wild-type embryos (D), embryos with no Dl (E), and no terminal signaling (F).

(G and H) The model can also predict *zen* expression pattern in multiple genetic backgrounds. The model predicts ectopic expression pattern of *zen* in the absence of anterior substrates of MAPK (G) and posterior expression in embryos with uniform nuclear of Dl (H).

accumulation of ectopically expressed Yan as a Cic-independent reporter of MAPK activity. Similar to Cic, Yan is degraded in response to MAPK phosphorylation (Figure S2) (Lai and Rubin, 1992; Rebay and Rubin, 1995). We found that the spatial pattern of Yan downregulation is also asymmetric: nuclear levels of Yan at the anterior pole were higher than at the posterior pole (Figure 1G). This suggests that MAPK activity toward all of its uniformly distributed substrates is lower in this region of the embryo.

According to our model, *zen* repression requires a critical value of both Dl, distributed in a ventral-to-dorsal pattern, and R, distributed in an AP pattern. To find this pattern, we used an enzyme kinetics model where anteriorly localized substrates of E competitively inhibit R downregulation at the poles. Starting from the experimentally observed shape of the nuclear Dl gradient (Chung et al., 2011; Kanodia et al., 2009), the AP asymmetry of Cic downregulation (Kim et al., 2010), and the expression boundary of *zen* in the midbody of the embryo (Chung et al., 2011), we derived an analytical expression that describes *zen* expression boundary on the surface of a spheroid that approximates the three-dimensional shape of the embryo (see Experimental Procedures for a more detailed presentation of the model).

Remarkably, this simple model can account for changes of *zen* expression in response to multiple perturbations of maternal patterning systems (Figures 2D–2H). For instance, removal of anterior MAPK substrates leads to ectopic *zen* expression at the anterior pole (Figure 2G), making the pattern symmetric along the AP axis. This model also successfully predicts the persistence of *zen* expression at the posterior pole of embryos with uniform nuclear Dl (Figure 2H), in agreement with *zen* expression in embryos derived from *cactus* mutant females (Rushlow et al., 1987). Thus, this model parsimoniously explains how *zen* expression changes in multiple mutant backgrounds. Finally, this model makes a number of predictions, which motivated our experiments presented below.

Experimental Tests of Model Predictions

A substrate competition model for *zen* regulation predicts that *zen* expression should become symmetric in embryos that lack anteriorly localized MAPK substrates (Figure 2G). To test this prediction, we examined *zen* expression in embryos that lack both Bcd and maternally contributed Hb, which is also distributed in an AP pattern and phosphorylated by MAPK. In these embryos, both MAPK phosphorylation and signaling activity, reported by Cic downregulation, are essentially symmetric (Figures 3C and 3D). Furthermore, a target gene of MAPK signaling, *tailless* (*tll*), is expressed as two symmetric caps at the poles (Figure 3F). Thus, MAPK signaling and its transcriptional effects are indeed symmetric in these embryos. Importantly, *zen* expression also becomes symmetric (Figures 3H–3J and S3B–S3D).

These observations are consistent with the notion that the AP asymmetry of the wild-type *zen* expression pattern is generated by anteriorly localized MAPK substrates. Furthermore, these observations suggest that Bcd and Hb constitute a significant fraction of all MAPK substrates as the anterior pole. Moreover, loss of *bcd* alone increases *zen* expression at the anterior pole (Figures 4N–4P). Thus, removal of a single binding partner of MAPK can generate a significant downstream effect in a larger patterning network.

Another prediction of our model is that the inhibitory effects of Bcd on MAPK signaling and *zen* expression do not depend on its transcriptional activity. To test this prediction, we used Bcd-A_9, a (K50L) form of Bcd that does not bind to Bcd's DNA recognition sequences and thus cannot activate endogenous transcriptional targets of Bcd (Hanes et al., 1994). We found that expression of two copies of this construct, driven by Bcd endogenous promoter in the *bcd* homozygous embryos (*Bcd-A_9;bcd*), does not activate several *bcd* targets (Figures 4E–4H), yet does rescue both MAPK phosphorylation and Cic downregulation gradients (Figures 4A–4D). Importantly, *zen* expression is greatly reduced at the anterior pole in these embryos (Figures 4J–4L). Thus,

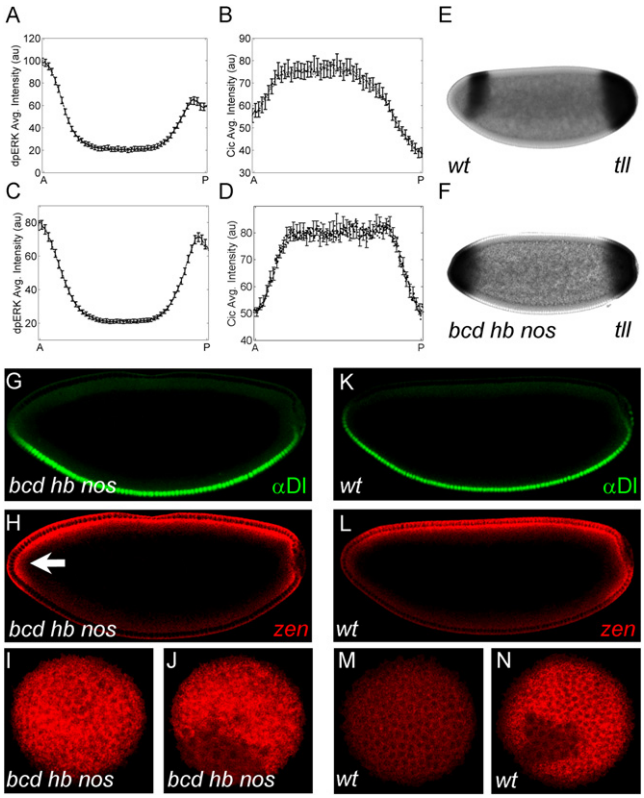

Figure 3. Anterior Repression of *zen* Requires Bcd and Hb

(A and B) Quantified gradient of MAPK phosphorylation (A) and Cic downregulation (B) in wild-type embryos (n = 27 for A and n = 29 for B; error bars are SEM). Cic downregulation gradient is reproduced from Figure 1F.

(C and D) Quantified gradients of MAPK phosphorylation (C) and Cic downregulation (D) in embryos derived from *bcd hb nos* germline clone flies (n = 34 for both gradients; error bars are SEM). The anterior and posterior levels of both MAPK phosphorylation and nuclear Cic are nearly symmetric ($p > 0.1$).

(E and F) Expression of *tll* in wild-type (E) and *bcd hb nos* (F) embryos.

(G and H) Dl protein and *zen* mRNA in a *bcd hb nos* embryo. In the absence of Bcd, Hb, and Nos, *zen* is expressed throughout the anterior pole (arrow).

(I and J) Optical images of *zen* at the anterior (I) and posterior (J) poles. Similar to Figure 3H, *zen* is expressed at both poles in the absence of anterior substrates of MAPK.

(K and L) Dl protein and *zen* mRNA in a wild-type embryo.

(M and N) End-on images of *zen* mRNA at the anterior (M) and posterior (N) poles of wild-type embryos.

transcriptionally inert Bcd can inhibit MAPK-dependent downregulation of Cic, and this effect propagates to the Dl-dependent gene expression.

Another argument supporting our model of gene regulation by MAPK substrate competition is based on the analysis of the expression of *hb*, which is transcriptionally regulated by both anterior and terminal systems. In embryos derived from *bcd* homozygous flies, *hb* is expressed at the poles, reflecting its activation by the terminal system (Margolis et al., 1995). However, the anterior domain of this pattern is eliminated by expressing two copies of *Bcd-A*$_9$ (Figure 4F). This suggests that transcriptionally inert Bcd weakens terminal signaling at the anterior region, leading to a drastic reduction of the anterior *hb* expression. This conclusion is further strengthened by the fact that, in the same background, the anterior expression of *hkb* and *tll*, both of which depend on MAPK signaling, is also attenuated, even when compared to their expression in embryos derived from *bcd* homozygous females (Figure 4H; data not shown).

Taken together with the wild-type pattern of *zen* expression and its changes in mutant backgrounds, our results support a nontranscriptional mechanism, according to which the anterior repression of *zen* depends on competitive inhibition of Cic downregulation by anteriorly localized MAPK substrates. Although our proof of this mechanism is not exhaustive, we cannot formulate a viable alternative that would have a similar explanatory and predictive power. For instance, we could rule out the alternative models that rely on the AP asymmetry of the Dl gradient or on the more indirect, transcriptional, effect of the terminal system (see Figures S4A–S4H).

DISCUSSION

Patterning of the anterior region of the *Drosophila* embryo depends on the concentration gradient of Bcd, the nuclear localization gradient of Dl, and the phosphorylation gradient of MAPK (Casanova, 1990; Driever and Nüsslein-Volhard, 1988; Rushlow et al., 1989; St Johnston and Nüsslein-Volhard, 1992). Previous studies revealed several pairwise interactions between these signals (Pignoni et al., 1992; Ronchi et al., 1993; Rusch and Levine, 1994). In particular, Bcd and Dl synergistically regulate a large number of genes by binding to common *cis*-regulatory regions of those genes (Papatsenko et al., 2009). Similarly, the concentration gradient of Cic, established by MAPK signaling, controls the posterior expression borders of genes activated by Bcd (Löhr et al., 2009).

We discovered an additional, ternary interaction of the AP, DV, and terminal systems. This mechanism cannot be reduced to a particular regulatory region on DNA or to a single protein. Instead, it is based on competitive effects in a network formed by MAPK and its substrates. Based on the asymmetry of the wild-type pattern of *zen* mRNA, we propose that the anteriorly localized substrates of MAPK act as competitive inhibitors in the process of MAPK-dependent gene derepression. The same mechanism can regulate other genes that are repressed by the Dl gradient. For example, *decapentaplegic* (*dpp*), another gene expressed in the dorsal region, is regulated by the joint action of the DV and terminal systems (Casanova, 1991; Huang et al., 1993). Similar to *zen*, the expression of *dpp* is weaker at the anterior pole than at the posterior (data not shown).

At this point, the main evidence supporting the notion that MAPK substrate competition controls gene expression in the embryo is provided by experiments that perturb the expression levels of MAPK substrates. In the future, we plan to complement these experiments by perturbations of the docking domains involved in MAPK interactions with its binding partners (Torii et al., 2004; Shaul and Seger, 2007; Goldsmith et al., 2007; Bardwell, 2006). For instance, according to our model, the spatial pattern of *zen* should become symmetric in embryos in which the wild-type Bcd protein is replaced by a Bcd variant that lacks MAPK docking domain. To test this prediction, we plan to identify the docking domains involved in MAPK/Bcd and other MAPK-dependent interactions in the early embryo.

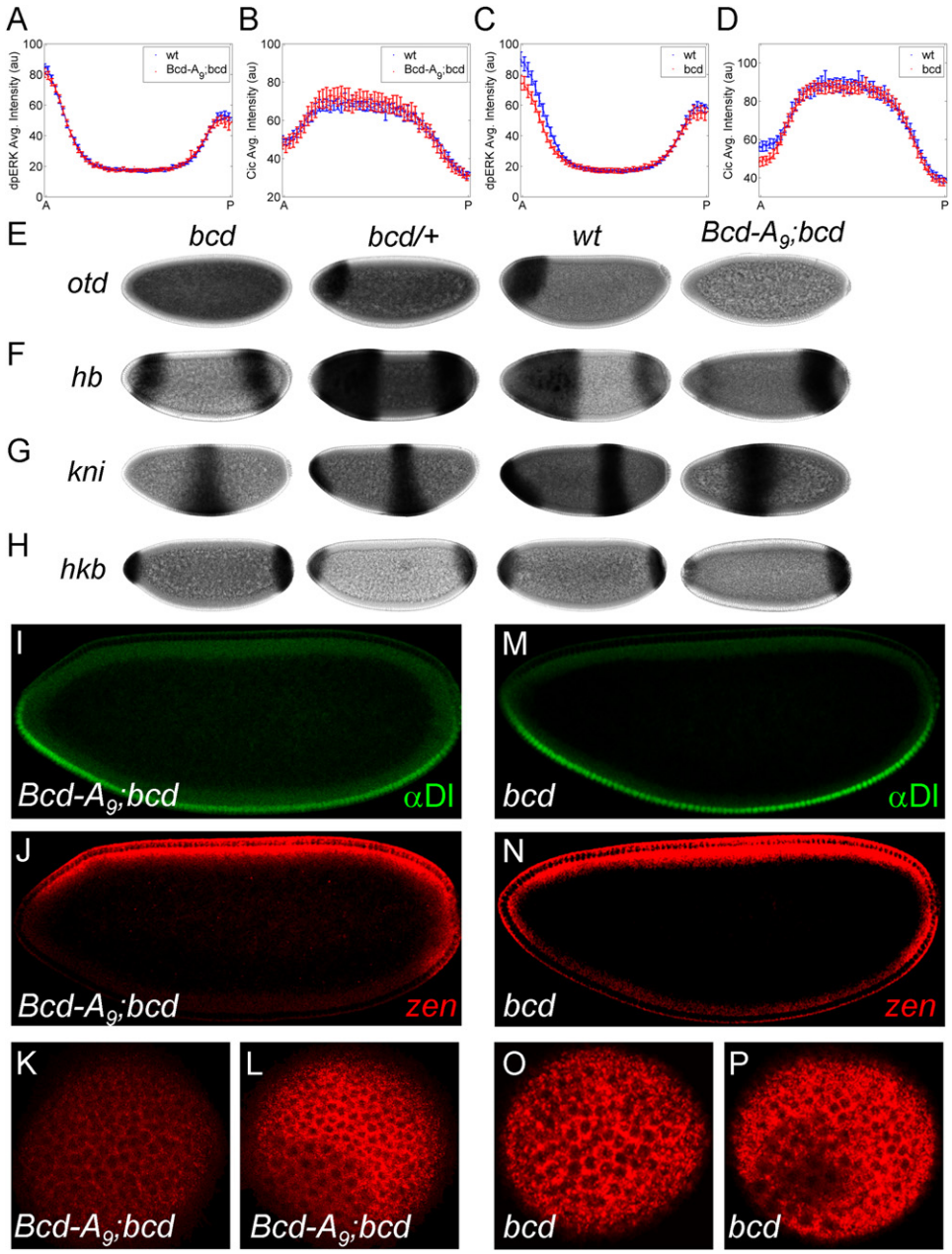

Figure 4. Anterior Repression of *zen* Does Not Require Transcriptional Activity of Bcd

(A and B) Expression of two copies of *Bcd-A$_9$* construct driven by Bcd promoter in the *bcd* null embryos (*Bcd-A$_9$;bcd*) results in MAPK phosphorylation (A) and nuclear Cic (B) gradients that are indistinguishable from those in wild-type embryo (error bars are SEM). The numbers of embryos used in the analysis are: $N_{WT} = 32$, $N_{mutant} = 19$ for (A) and $N_{WT} = 28$, $N_{mutant} = 24$ for (B).

(C and D) Quantified gradients of MAPK phosphorylation (C) and Cic downregulation (D) in *bcd* null embryos (error bars are SEM). $N_{WT} = 28$, $N_{mutant} = 28$ for (C) and $N_{WT} = 39$, $N_{mutant} = 38$ for (D).

(E–H) Expression of *otd* (E), *hb* (F), *kni* (G), and *hkb* (H) in embryos derived from *bcd* homozygous (first column), *bcd* heterozygous (second column), wild-type (third column), and *bcd* homozygous with *Bcd-A$_9$* (fourth column) flies. Anterior expression of these genes is significantly reduced in *Bcd-A$_9$;bcd* embryos.

(I and J) Nuclear Dl and *zen* mRNA in a *Bcd-A$_9$;bcd* embryo: similar to wild-type embryos, *zen* is repressed at the anterior pole.

(K and L) *zen* expressions at the anterior (K) and posterior (L) poles also show that *zen* is not expressed at the anterior pole in this mutant background.

(M and N) Nuclear Dl and *zen* mRNA in a *bcd* null embryo.

(O and P) *zen* expression at the anterior (O) and posterior (P) poles of embryos from *bcd* null flies.

Identification of these domains should shed light on the functional significance of MAPK substrate competition in the early embryo and other stages of development.

Competitive effects are likely to be a general feature of biomolecular networks, which are commonly organized around hubs, regulators that can interact with a large number of targets.

For instance, in posttranscriptional regulation by microRNAs, different targets of a given microRNA can compete for their common regulator. Indeed, a number of recent studies suggest that mRNA competition in microRNA networks can lead to indirect inhibitory interactions between transcripts (Ebert et al., 2007). As a consequence, a given mRNA can control translation of other transcripts by regulating activity of their common microRNAs, in a way that is independent of its protein-coding function (Poliseno et al., 2010). Exploring network-level consequences of such effects requires a quantitative approach, similar to the one used in our study of MAPK signaling in *Drosophila* embryo.

EXPERIMENTAL PROCEDURES

In Situ Hybridization and Immunohistochemistry

Fluorescence in situ hybridization (FISH) was performed as described elsewhere (Kosman et al., 2004). Embryos were dechorionated in 50% bleach and fixed in 8% formaldehyde in PBS for 20 min. Embryos were then incubated in 90% xylene for 1 hr and then treated with 80% acetone for 10 min at −20°C. Next, embryos were hybridized overnight at 60°C with antisense probes labeled with digoxigenin (DIG) or fluorescein. Embryos with labeled probes were visualized using standard immunofluorescence technique. The following primary antibodies were used in this study: sheep anti-DIG (Roche; 1:200), mouse anti-dpERK (Sigma; 1:100), mouse anti-Dorsal (DSHB; 1:100), rabbit anti-Cic (see Supplemental Experimental Procedures; 1:2000), mouse anti-Yan (DSHB; 1:100), rat anti-Hkb (Ashyraliyev et al., 2009), and rabbit anti-fluorescein (Invitrogen; 1:200). The Alexa Fluor-conjugated secondary antibodies were from Invitrogen (1:500). DAPI (1:10,000; Vector Laboratories) was used to visualize nuclei.

Microscopy and Image Processing

Imaging was done on a Zeiss LSM510 confocal microscope, with a Zeiss C-Apo 20× objective (NA = 0.6). High-resolution images (512 × 512 pixels, 12 bits depth) were obtained from a focal plane in the mid-horizontal cross section of the embryo. Images of individual embryos were automatically extracted from raw confocal files and reoriented as described elsewhere (Coppey et al., 2008). For end-on imaging, embryos were oriented using previously described microfluidic device (Chung et al., 2011). Zeiss LSM510 confocal microscope with a C-Apo 40× water-immersion objective (NA = 1.2) was used for end-on imaging.

Gradient Quantification and Statistical Analysis

Quantification of spatial gradients of a protein of interest (dpERK, Cic, or Yan) was performed as described previously (Coppey et al., 2008). Confocal images of embryos stained with antibodies detecting the protein of interest were analyzed using a custom-made MATLAB image processing program. A Student's t test was used to determine the statistical significance in the asymmetry of Cic and Yan gradients. Briefly, a quantified gradient from a single embryo was first separated into anterior and posterior regions; these two regions were then independently approximated by a Gaussian with negative normalization (constant minus a Gaussian). The minima of the two fitted curves provide the anterior and posterior levels of Cic (or Yan) in this embryo. This process was repeated for gradients extracted from 20–30 embryos. A Student's t test was used to test whether the mean of this sample is significantly different from one.

Mathematical Model of *zen* Regulation

We explain our model using a rectangular embryo, where the x and y directions represent the AP and DV axes of the actual embryo. We assume that the AP and terminal signals are uniform along the DV axis. The rectangular case is presented here for simplicity because it contains all of the essential features of our model, and leads to a simple algebraic expression that describes the boundary of *zen* expression. The same model applies for an embryo shaped as a prolate spheroid and was used to generate images in Figure 2.

Let R denote a factor, such as Cic, that acts together with Dl to repress *zen*. The joint repressive action of Dl and R can be modeled by the product of Dl and R concentrations, Dl*R. In the model, *zen* is expressed when this product is below some threshold, denoted by Θ. Thus, the level of *zen* expression, denoted by Z, is given by $Z(x,y) = H(\Theta - Dl(y)\times R(x))$, where $H(u)$ is the Heaviside step function: $H(u) = 1$, when $u>0$ and zero otherwise. The boundary of *zen* expression, denoted by $y_Z(x)$, is then given by the implicit function: $\Theta = Dl(y)\times R(x)$. This equation can be related to the experimentally observed profiles of the Bcd, Dl, and Cic gradients.

We assume that repressor R is produced at a constant rate, denoted by S_R, and degraded via two parallel channels: constitutive degradation throughout the embryo and faster degradation that depends on the terminal signal. A steady-state model for repressor level then becomes $S_R = k_c R + V(R)$, where k_c is the rate constant of constitutive degradation, and $V(R)$ is the rate law for the enzymatic degradation that depends on the terminal signal. We assume that the spatial pattern of active enzyme, denoted by $E(x)$ (phosphorylated MAPK), is uniform along the DV axis. The spatial pattern of enzyme distribution $E(x)$ is given by the product of the amplitude E_0 and a symmetric function $f_E(x)$ that is equal to one at the poles and close to zero in the middle of embryo.

We assume that degradation of R follows Michaelis-Menten kinetics, with constants k_{cat} and K_M. We also assume that Bcd competitively inhibits MAPK-dependent repressor degradation. This leads to the following expression for the rate of signal-induced repressor degradation: $V(R) = k_{cat}E(x)R(x)/(K_M + R(x) + K_M B(x)/K_I)$, where K_I is the equilibrium constant of enzyme-Bcd interaction.

To simplify the algebra, we assume that the enzyme is not saturated by R. Under this assumption, $V(R) = k_{cat}E(x)R/K_M(1 + B(x)/K_I)$. Substituting this into the mass balance for repressor levels, we get the following expression for the spatial pattern of R:

$$R(x) = \frac{S/k_c}{(1 + \alpha f_E(x)/(1 + f_B(x)\beta))},$$

where α and β are defined as: $\alpha = k_{cat}E_0/k_c K_M$, $\beta = B_0/K_I$. These parameters can be estimated from the wild-type pattern of Cic downregulation: At the posterior pole, where $f_E(x) = 1$, but the concentration of anteriorly localized Bcd is zero ($f_B(x) = 0$), Cic is downregulated to 10% of its level in the midbody of the embryo, where $f_E(x) = 0$. From this result, we find that $\alpha \approx 9$. At the same time, at the anterior of the embryo, where $f_B(u) = 1$, Cic is downregulated only to ~50% of its midbody level. Based on this result, and on the estimate for α, we get that $\beta \approx 4$. Combining these estimates with the shape of the Bcd gradient and the shape of the terminal signal, we can predict how R is distributed throughout the AP axis of the embryo.

The equation for the boundary of *zen* expression then takes the following form:

$$D_0 f_D(y) \times \frac{S/k_c}{(1 + \alpha f_E(x)/(1 + f_B(x)\beta))} = \Theta,$$

where D_0 is the amplitude of the nuclear Dl gradient and $f_D(y)$ is the shape that characterizes its distribution along the embryo.

Introducing one more dimensionless group $\gamma \equiv \Theta k_c/(S\times D_0)$, we get the following equation for the *zen* expression boundary:

$$\frac{f_D(y)}{1 + \alpha f_E(x)/(1 + \beta f_B(x))} = \gamma.$$

The remaining parameter of the model, γ, can be estimated from the location of the *zen* boundary in the midbody region of the embryo, where $f_E(x) \approx 0$, which implies that $\gamma = f_D(y_{Z,m})$, where $y_{Z,m}$ denotes the position of the *zen* boundary at the midbody region of the embryo. Based on our previous imaging results (Chung et al., 2011; Kanodia et al., 2009), we estimate that $\gamma \approx 0.1$.

Putting everything together, we get the following equation for the expression boundary of the wild-type pattern:

$$\frac{f_D(y)}{(1 + 9 f_E(x)/(1 + 4 f_B(x)))} = 0.1.$$

Note that the values of the three dimensionless groups in the model were obtained from the asymmetries of the wild-type pattern of Cic downregulation, the location of the *zen* expression boundary in the midbody region of the embryo, and the spatial distribution of the nuclear Dl gradient in the midbody region.

We can now combine the values of α, β, and γ with the empirically determined distributions for the patterning signals, $f_D(y)$, $f_E(x)$, and $f_B(x)$, to plot the wild-type pattern of *zen* expression. This model predicts how the *zen* expression boundary "bends" in response to variations in the levels of anterior, terminal, and DV signals. For example, removing Bcd makes MAPK more available for *R*, lowering a corepressor that acts together with Dl in *zen* repression, and results in ectopic *zen* at the anterior pole (Figure 2G).

SUPPLEMENTAL INFORMATION

Supplemental Information includes four figures and Supplemental Experimental Procedures and can be found with this article online at doi:10.1016/j.devcel.2011.05.009.

ACKNOWLEDGMENTS

We thank Ze'ev Paroush, Eric Wieschaus, Mathieu Coppey, Oliver Grimm, Trudi Schüpbach, Christine Rushlow, Ulrike Löhr, and members of the Shvartsman laboratory for multiple helpful discussions. We thank Trudi Schüpbach, Christine Rushlow, Natalie Dostatni, Steve Hanes, Johannes Jaeger, Kim Rittenhouse, and Oliver Grimm for reagents used in this work. S.Y.S. acknowledges partial support by NSF via grant DMS-0718604, as well as P50 GM071508 and RO1 GM078079 grants from the NIH. G.J. acknowledges support by ICREA by grants from MICINN (BFU2008-01875) and AGAUR (2009SGR-1075). H.L. was supported by NSF DBI-0649833, NIH NS058465, Sloan Foundation, and DuPont Foundation. C.A.B. was supported by R01-GM45248 grant from the NIH.

Received: October 20, 2010
Revised: March 19, 2011
Accepted: May 12, 2011
Published: June 13, 2011

REFERENCES

Ajuria, L., Nieva, C., Winkler, C., Kuo, D., Samper, N., Andreu, M.J., Helman, A., González-Crespo, S., Paroush, Z., Courey, A.J., and Jiménez, G. (2011). Capicua DNA-binding sites are general response elements for RTK signaling in *Drosophila*. Development *138*, 915–924.

Ashyraliyev, M., Siggens, K., Janssens, H., Blom, J., Akam, M., and Jaeger, J. (2009). Gene circuit analysis of the terminal gap gene huckebein. PLoS Comput. Biol. *5*, e1000548.

Astigarraga, S., Grossman, R., Díaz-Delfín, J., Caelles, C., Paroush, Z., and Jiménez, G. (2007). A MAPK docking site is critical for downregulation of Capicua by Torso and EGFR RTK signaling. EMBO J. *26*, 668–677.

Bardwell, L. (2006). Mechanisms of MAPK signalling specificity. Biochem. Soc. Trans. *34*, 837–841.

Casanova, J. (1990). Pattern formation under the control of the terminal system in the *Drosophila* embryo. Development *110*, 621–628.

Casanova, J. (1991). Interaction between torso and dorsal, two elements of different transduction pathways in the *Drosophila* embryo. Mech. Dev. *36*, 41–45.

Casanova, J., Furriols, M., McCormick, C.A., and Struhl, G. (1995). Similarities between trunk and spätzle, putative extracellular ligands specifying body pattern in *Drosophila*. Genes Dev. *9*, 2539–2544.

Chung, K., Kim, Y., Kanodia, J.S., Gong, E., Shvartsman, S.Y., and Lu, H. (2011). A microfluidic array for large-scale ordering and orientation of embryos. Nat. Methods *8*, 171–176.

Coppey, M., Boettiger, A.N., Berezhkovskii, A.M., and Shvartsman, S.Y. (2008). Nuclear trapping shapes the terminal gradient in the *Drosophila* embryo. Curr. Biol. *18*, 915–919.

Doyle, H.J., Kraut, R., and Levine, M. (1989). Spatial regulation of zerknüllt: a dorsal-ventral patterning gene in *Drosophila*. Genes Dev. *3*, 1518–1533.

Driever, W., and Nüsslein-Volhard, C. (1988). The bicoid protein determines position in the *Drosophila* embryo in a concentration-dependent manner. Cell *54*, 95–104.

Dubnicoff, T., Valentine, S.A., Chen, G., Shi, T., Lengyel, J.A., Paroush, Z., and Courey, A.J. (1997). Conversion of dorsal from an activator to a repressor by the global corepressor Groucho. Genes Dev. *11*, 2952–2957.

Ebert, M.S., Neilson, J.R., and Sharp, P.A. (2007). MicroRNA sponges: competitive inhibitors of small RNAs in mammalian cells. Nat. Methods *4*, 721–726.

Gabay, L., Seger, R., and Shilo, B.Z. (1997). MAP kinase in situ activation atlas during *Drosophila* embryogenesis. Development *124*, 3535–3541.

Goff, D.J., Nilson, L.A., and Morisato, D. (2001). Establishment of dorsal-ventral polarity of the *Drosophila* egg requires capicua action in ovarian follicle cells. Development *128*, 4553–4562.

Goldsmith, E.J., Akella, R., Min, X., Zhou, T., and Humphreys, J.M. (2007). Substrate and docking interactions in serine/threonine protein kinases. Chem. Rev. *107*, 5065–5081.

Hanes, S.D., Riddihough, G., Ish-Horowicz, D., and Brent, R. (1994). Specific DNA recognition and intersite spacing are critical for action of the bicoid morphogen. Mol. Cell. Biol. *14*, 3364–3375.

Huang, J.D., Schwyter, D.H., Shirokawa, J.M., and Courey, A.J. (1993). The interplay between multiple enhancer and silencer elements defines the pattern of decapentaplegic expression. Genes Dev. *7*, 694–704.

Janody, F., Sturny, R., Catala, F., Desplan, C., and Dostatni, N. (2000). Phosphorylation of bicoid on MAP-kinase sites: contribution to its interaction with the torso pathway. Development *127*, 279–289.

Jiang, J., Cai, H., Zhou, Q., and Levine, M. (1993). Conversion of a dorsal-dependent silencer into an enhancer: evidence for dorsal corepressors. EMBO J. *12*, 3201–3209.

Jiménez, G., Guichet, A., Ephrussi, A., and Casanova, J. (2000). Relief of gene repression by torso RTK signaling: role of capicua in *Drosophila* terminal and dorsoventral patterning. Genes Dev. *14*, 224–231.

Kanodia, J.S., Rikhy, R., Kim, Y., Lund, V.K., DeLotto, R., Lippincott-Schwartz, J., and Shvartsman, S.Y. (2009). Dynamics of the Dorsal morphogen gradient. Proc. Natl. Acad. Sci. USA *106*, 21707–21712.

Kim, Y., Coppey, M., Grossman, R., Ajuria, L., Jiménez, G., Paroush, Z., and Shvartsman, S.Y. (2010). MAPK substrate competition integrates patterning signals in the *Drosophila* embryo. Curr. Biol. *20*, 446–451.

Kosman, D., Mizutani, C.M., Lemons, D., Cox, W.G., McGinnis, W., and Bier, E. (2004). Multiplex detection of RNA expression in *Drosophila* embryos. Science *305*, 846.

Lai, Z.C., and Rubin, G.M. (1992). Negative control of photoreceptor development in *Drosophila* by the product of the yan gene, an ETS domain protein. Cell *70*, 609–620.

Liang, H.L., Nien, C.Y., Liu, H.Y., Metzstein, M.M., Kirov, N., and Rushlow, C. (2008). The zinc-finger protein Zelda is a key activator of the early zygotic genome in *Drosophila*. Nature *456*, 400–403.

Löhr, U., Chung, H.R., Beller, M., and Jäckle, H. (2009). Antagonistic action of Bicoid and the repressor Capicua determines the spatial limits of *Drosophila* head gene expression domains. Proc. Natl. Acad. Sci. USA *106*, 21695–21700.

Margolis, J.S., Borowsky, M.L., Steingrímsson, E., Shim, C.W., Lengyel, J.A., and Posakony, J.W. (1995). Posterior stripe expression of hunchback is driven from two promoters by a common enhancer element. Development *121*, 3067–3077.

Maslov, S., and Ispolatov, I. (2007). Propagation of large concentration changes in reversible protein-binding networks. Proc. Natl. Acad. Sci. USA *104*, 13655–13660.

Papatsenko, D., Goltsev, Y., and Levine, M. (2009). Organization of developmental enhancers in the *Drosophila* embryo. Nucleic Acids Res. *37*, 5665–5677.

Pignoni, F., Steingrímsson, E., and Lengyel, J.A. (1992). bicoid and the terminal system activate tailless expression in the early *Drosophila* embryo. Development *115*, 239–251.

Poliseno, L., Salmena, L., Zhang, J., Carver, B., Haveman, W.J., and Pandolfi, P.P. (2010). A coding-independent function of gene and pseudogene mRNAs regulates tumour biology. Nature *465*, 1033–1038.

Ratnaparkhi, G.S., Jia, S., and Courey, A.J. (2006). Uncoupling dorsal-mediated activation from dorsal-mediated repression in the *Drosophila* embryo. Development *133*, 4409–4414.

Rebay, I., and Rubin, G.M. (1995). Yan functions as a general inhibitor of differentiation and is negatively regulated by activation of the Ras1/MAPK pathway. Cell *81*, 857–866.

Ronchi, E., Treisman, J., Dostatni, N., Struhl, G., and Desplan, C. (1993). Down-regulation of the *Drosophila* morphogen bicoid by the torso receptor-mediated signal transduction cascade. Cell *74*, 347–355.

Rusch, J., and Levine, M. (1994). Regulation of the dorsal morphogen by the Toll and torso signaling pathways: a receptor tyrosine kinase selectively masks transcriptional repression. Genes Dev. *8*, 1247–1257.

Rushlow, C., Frasch, M., Doyle, H., and Levine, M. (1987). Maternal regulation of zerknüllt: a homoeobox gene controlling differentiation of dorsal tissues in *Drosophila*. Nature *330*, 583–586.

Rushlow, C.A., Han, K., Manley, J.L., and Levine, M. (1989). The graded distribution of the dorsal morphogen is initiated by selective nuclear transport in *Drosophila*. Cell *59*, 1165–1177.

Shaul, Y.D., and Seger, R. (2007). The MEK/ERK cascade: from signaling specificity to diverse functions. Biochim. Biophys. Acta *1773*, 1213–1226.

St Johnston, D., and Nüsslein-Volhard, C. (1992). The origin of pattern and polarity in the *Drosophila* embryo. Cell *68*, 201–219.

Torii, S., Nakayama, K., Yamamoto, T., and Nishida, E. (2004). Regulatory mechanisms and function of ERK MAP kinases. J. Biochem *136*, 557–561.